

## Supporting Information for

### The Cation- $\pi$ Interaction Enables a Halo-Tag Fluorogenic Probe for Fast No-Wash Live Cell Imaging and Gel-Free Protein Quantification

Yu Liu<sup>1</sup>, Kun Miao<sup>1</sup>, Noah P. Dunham<sup>2</sup>, Hongbin Liu<sup>3</sup>, Matthew Fares<sup>1</sup>, Amie K. Boal<sup>1,2</sup>,  
Xiaosong Li<sup>3</sup>, and Xin Zhang<sup>1,2,4\*</sup>

<sup>1</sup>Department of Chemistry, <sup>2</sup>Department of Biochemistry and Molecular Biology, <sup>4</sup>The Huck  
Institutes of the Life Sciences, The Pennsylvania State University, University Park, PA 16802

<sup>3</sup>Department of Chemistry, University of Washington, Seattle, WA 98105

\*Correspondence should be addressed to Xin Zhang ([xuz31@psu.edu](mailto:xuz31@psu.edu)).

#### **Table of contents**

Supplementary Figures S1-S15	pages S2-S16
Table S1-4	pages S17-S24
Synthetic Methods	pages S25-S36
Supplementary References	page S37

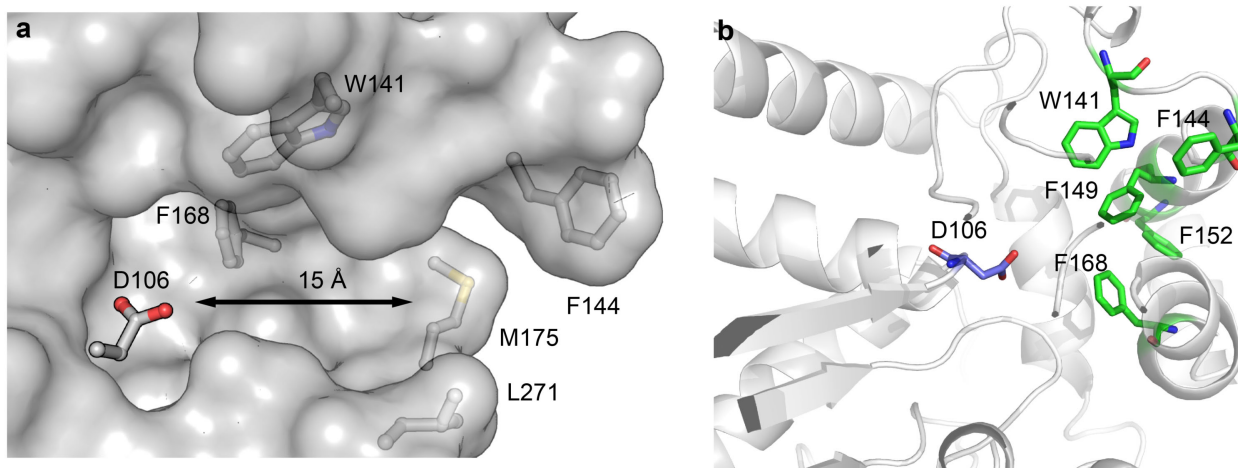


**Figure S1.** The 1.35 Å resolution crystal structure of the apo Halo-tag. **(a)** The 15 Å substrate binding tunnel separates the catalytic residue Asp 106 with the surface of the protein. **(b)** Aromatic residues (Trp 141, Phe 144, Phe 149, Phe 152, and Phe 168) are identified near the exit of the substrate binding tunnel.

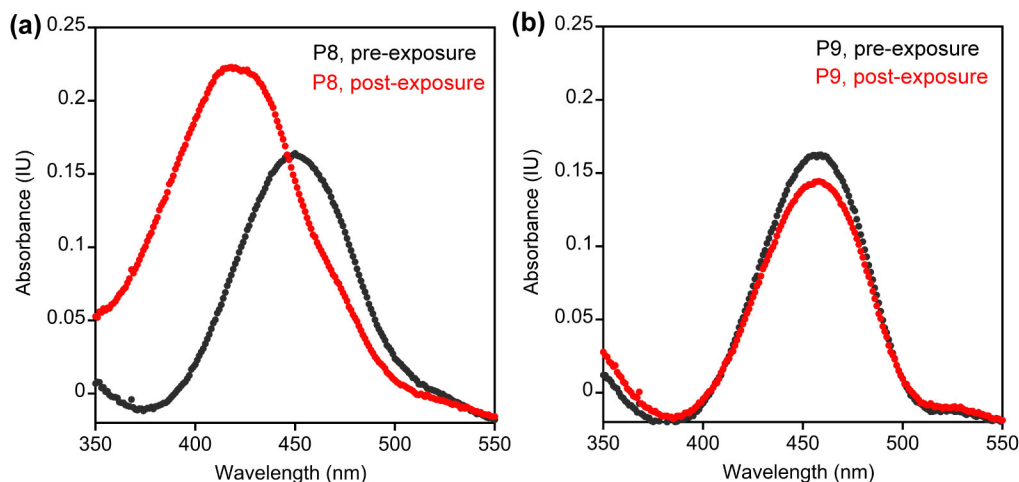


**Figure S2. The Halo-P9 conjugate is more photo-stable than the Halo-P8 conjugate.** (a) The UV absorbance maximum of a Halo-P8 conjugate shifted from 450 nm to 410 nm upon excitation with a 488 nm laser for 10 min, indicating that P8 is photo-labile. (b) The UV absorbance maximum of the Halo-P9 conjugate does not shift after laser irradiation for 10 min, indicating that P9 is resistant to photo-induced damage. The Halo-P8 and Halo-P9 conjugates were generated by incubating 50  $\mu$ M purified Halo protein with 20  $\mu$ M P8 or P9 in DPBS buffer for 30 min at 25  $^{\circ}$ C. Photoirradiation experiments were performed with a 488 nm laser (5 mW) for 10 min in quartz cuvettes. Absorbance spectra were recorded using an Agilent Cary-series UV-Vis spectrophotometer before and after photo-irradiation.

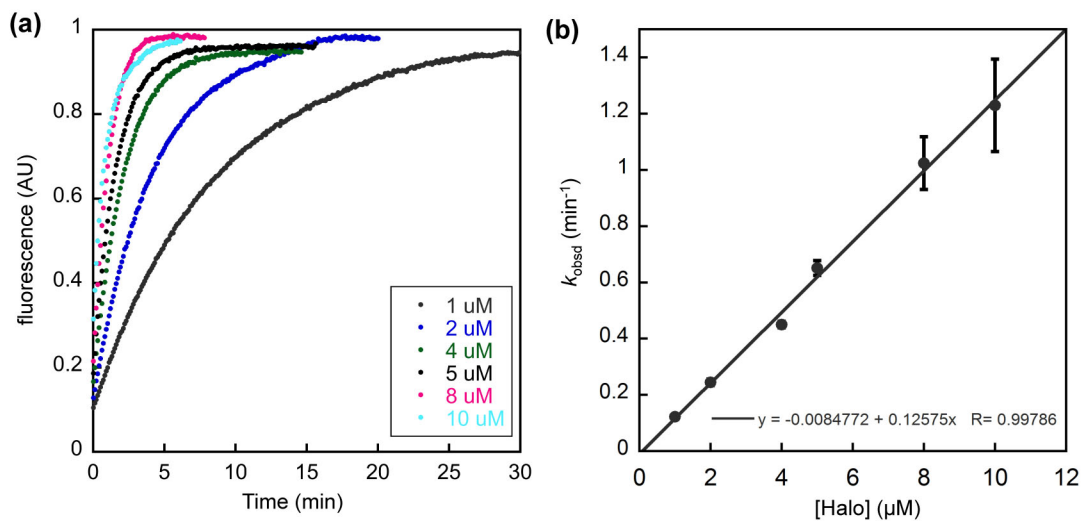


**Figure S3. *In vitro* labeling kinetics of P9 and Halo.** (a) Emission time course during reaction of P9 with Halo-tag. Reactions were carried out by mixing 0.5 μM P9 and increasing concentrations of the Halo-tag protein. The fluorescence intensity was followed at 530 nm with excitation at 450 nm. (b) The bimolecular rate constant is 2,100 M<sup>-1</sup>•s<sup>-1</sup>.

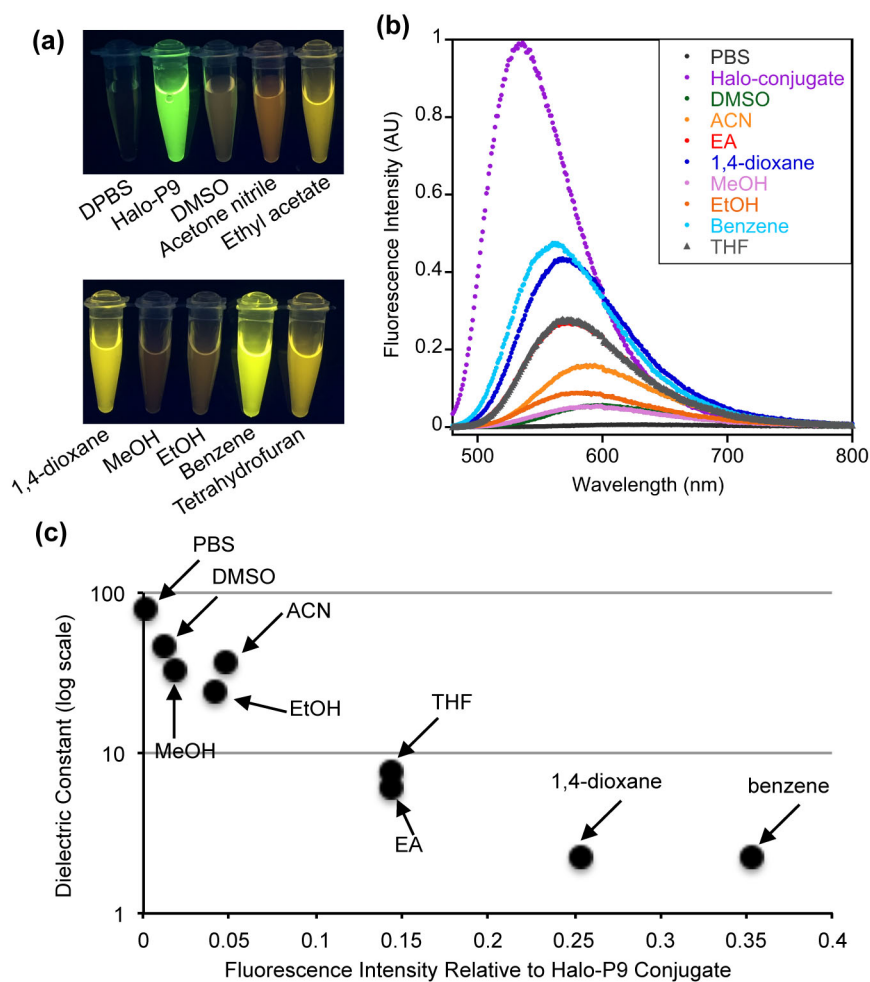


**Figure S4. Solvatochromism of P9.** (a) Images of P9 (20  $\mu\text{M}$ ) in solvents with various dielectric constants and image of the Halo-P9 conjugate in PBS buffer (20  $\mu\text{M}$  P9 and 50  $\mu\text{M}$  Halo). (b) Fluorescence emission spectra of P9 (20  $\mu\text{M}$ ) in different solvents and the Halo-P9 conjugate in PBS buffer (20  $\mu\text{M}$  P9 and 50  $\mu\text{M}$  Halo). Data were recorded by Tecan M1000Pro plate reader (excitation at 450 nm). (c) Increasing fluorescence intensities of P9 ( $E_m = 534$  nm) correlate with decreasing dielectric constant values. Dielectric constants of solvents used:  $\epsilon_{\text{benzene}} = 2.27$ ,  $\epsilon_{1,4\text{-dioxane}} = 2.25$ ,  $\epsilon_{\text{DMSO}} = 46.7$ ,  $\epsilon_{\text{ACN}} = 37.5$ ,  $\epsilon_{\text{EA}} = 6.02$ ,  $\epsilon_{\text{THF}} = 7.58$ ,  $\epsilon_{\text{MeOH}} = 32.7$ ,  $\epsilon_{\text{EtOH}} = 24.5$ ,  $\epsilon_{\text{PBS}} = 80.1$ .

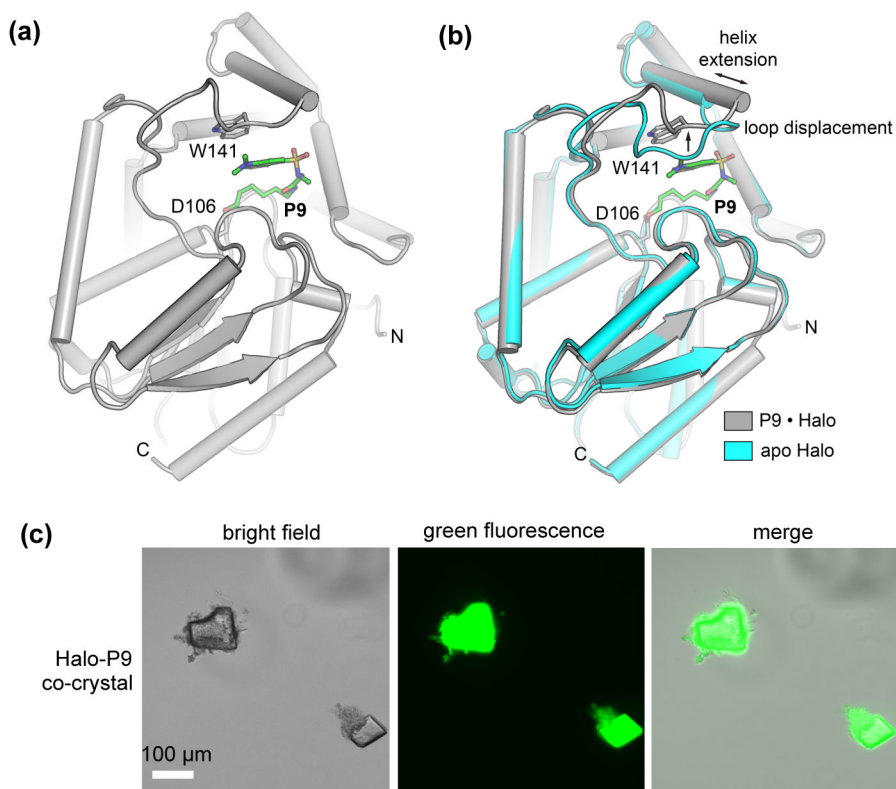


**Figure S5. The co-crystal structure of the Halo-P9 conjugate.** (a) A 1.92 Å resolution co-crystal structure of the Halo-P9 conjugate. P9 ligand (green) and selected amino acid residues (gray) are shown in ball-and-stick format and colored by atom type. (b) An overlay of the Halo-P9 conjugate (gray cartoon) with the apo Halo-tag structure (cyan cartoon) reveals little overall perturbation of the central fold to accommodate the ligand and a flip motion of a flexible loop accommodating Trp 141. However, a surface alpha helix is extended by a full turn to stabilize a displaced surface loop containing Trp 141. The fluorophore clashes with the aromatic side chain in the apo structure, suggesting that the loop refolds to position the indole moiety over the exocyclic dimethylamino group in P9. (c) The Halo-P9 co-crystal is fluorescent. The Halo-P9 crystals were looped out and transferred to a 35 mm glass bottom dish and images were taken by Biorad ZOE fluorescent cell imager. This data suggests that the dimethylamino group in the crystal structure should not be protonated in its ground state, because the positive charge of an electron donating group leads to non-fluorescence due to its lack of electron donating capacity.

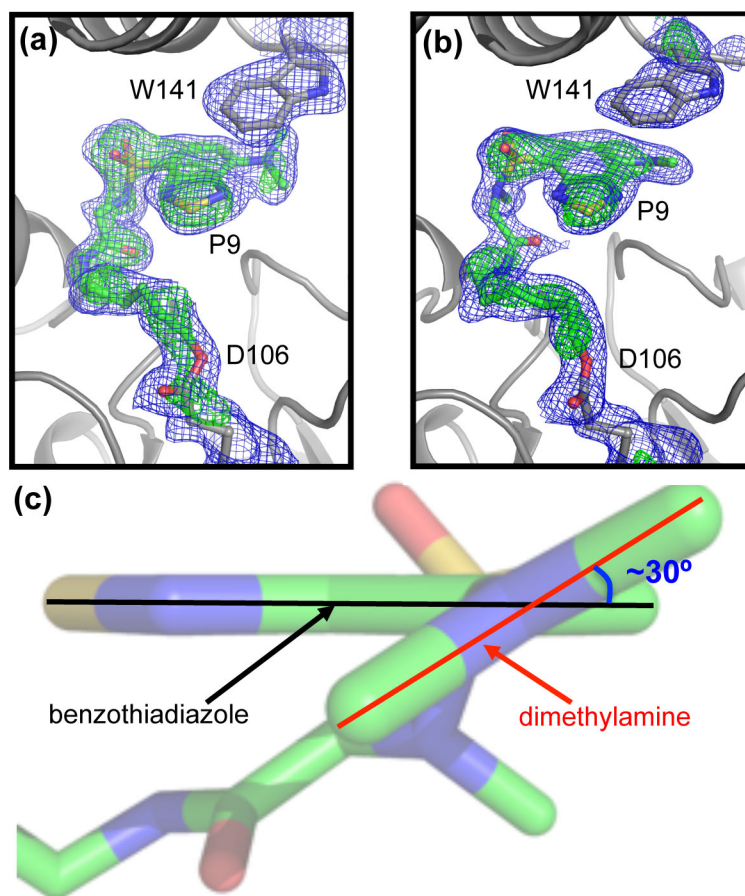


**Figure S6. Electron density map reveals detailed conformation of P9 in the Halo-P9 conjugate.** (a-b) A  $2F_o-F_c$  electron density map, contoured at  $1.5 \sigma$  (blue mesh), and  $F_o-F_c$  omit map, contoured at  $3.0 \sigma$  (green mesh) for the P9 ligand and selected amino acids in chain A (a) and chain B (b). (c) The dimethylamino group was positioned along a plane that was  $\sim 30^\circ$  tilted against the benzothiadiazole moiety.

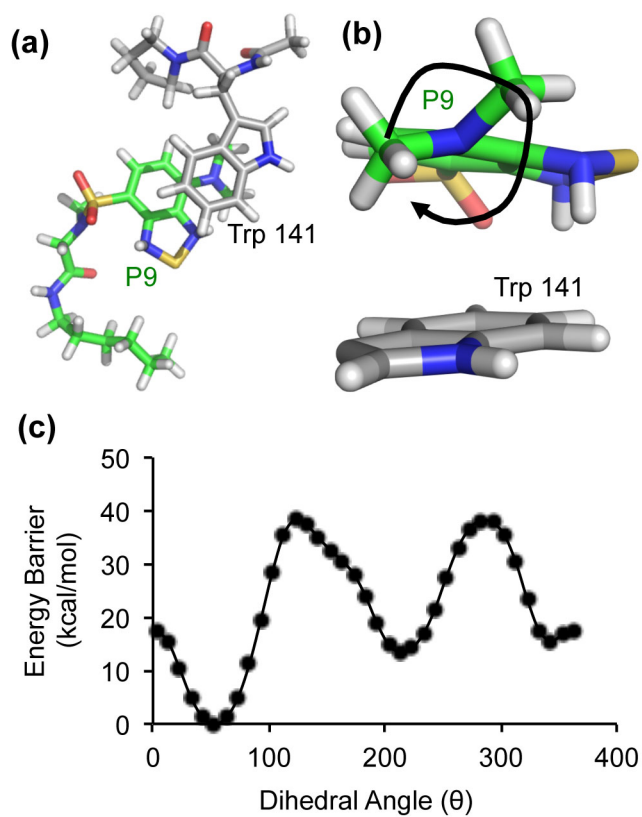


**Figure S7. A dihedral scan on the N-C bond verifies the sterically unfavorable twist of dimethyl-amino group of P9.** (a) The optimized geometry of the P9 • Trp 141 complex. (b) Position of the dimethylamino group positions in relative to the benzothiadiazole group. Black arrow indicates the rotation of the N-C bond in the dihedral scan, wherein the N atom refers to the dimethylamino group and the C atom belongs to the benzothiadiazole group. (c) The potential energy barrier for the dihedral rotation of the N-C bond.



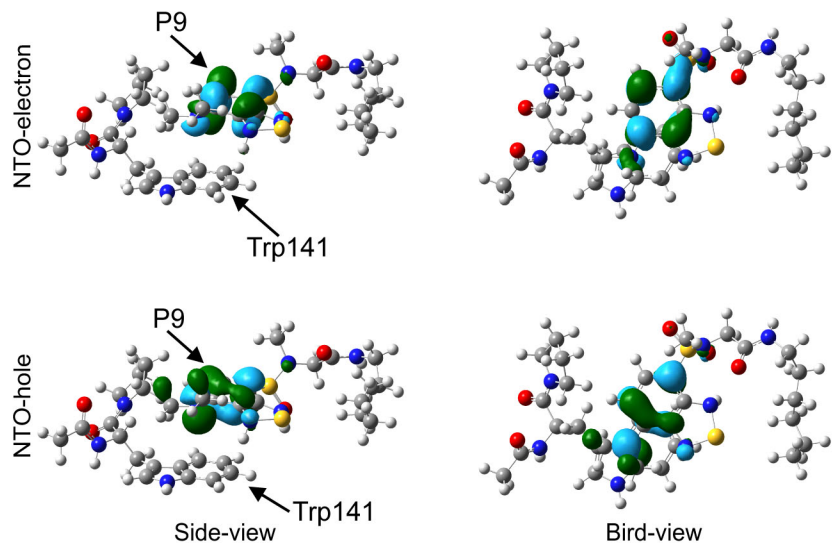


**Figure S8: The natural transition orbitals (plotted at isovalue 0.04) of the P9-Trp 141 complex upon  $S_3$  excitation using a TDDFT calculation.** The  $S_3$  state is found to be the brightest state upon vertical excitation. The natural transition orbitals show that the Trp 141 orbitals do not contribute to the  $S_3$  excitation. Thus, only the P9 electrons are in the excited state that contributes to fluorescence, whereas the Trp 141 electrons remain its ground state density.

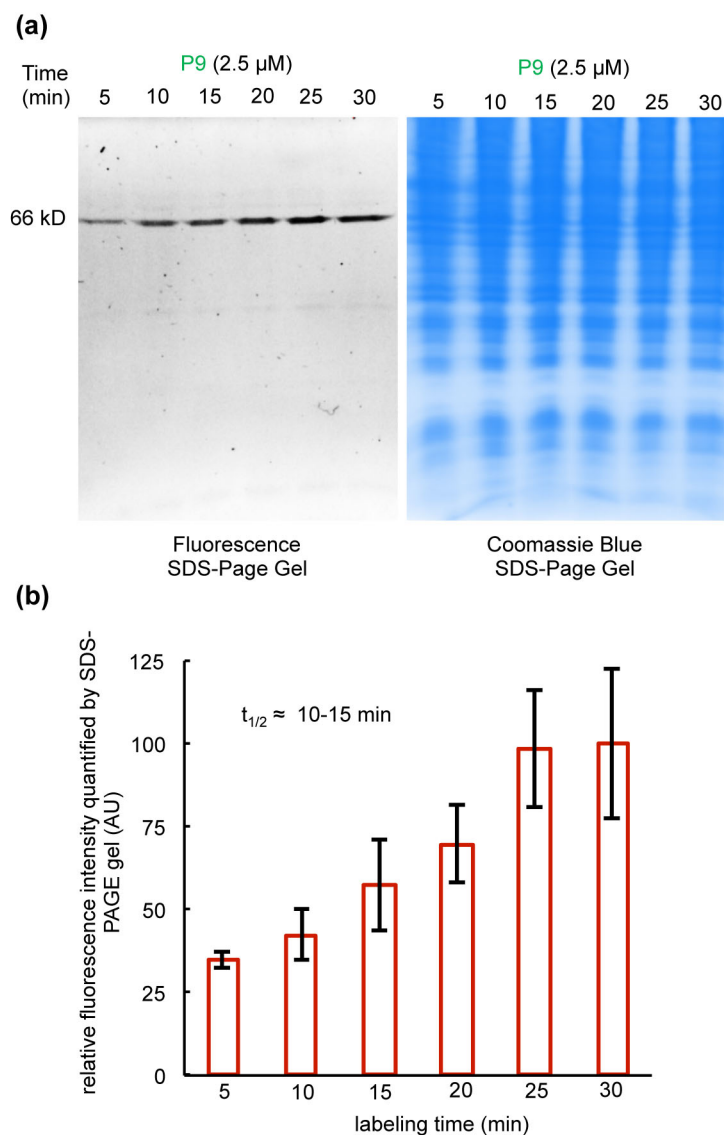


**Figure S9. Determination of half time for P9 (2.5  $\mu$ M) to label SOD1-Halo in HEK293T cells.** (a) The half time of P9 (2.5  $\mu$ M) to label SOD1-Halo was quantified by fluorescence SDS-Page gel. HEK293T cells were transiently transfected with SOD1-Halo for 24 h in 6-well plate. P9 (2.5  $\mu$ M) was introduced in the media at 0, 5, 10, 15, 20, 25 min and incubated at 37 °C. At 30 mins, cells were harvested and lysed by RIPA buffer and labeled as 30, 25, 20, 15, 10 and 5 min samples. Total protein concentration of all lysate samples were normalized by Bradford assay (0.1 mg/mL). Fluorescence and coomassie blue SDS-Page gels were scanned using Biorad Gel Doc EZ imager. Experiments were performed in biological triplicate. (b) Quantification of fluorescence intensity on gel. The half time for P9 (2.5  $\mu$ M) to label SOD1-Halo in HEK293T cells is estimated between 10 to 15 min. The saturation time is between 20 to 25 min. Error bars denote standard deviation from three independent experiments.

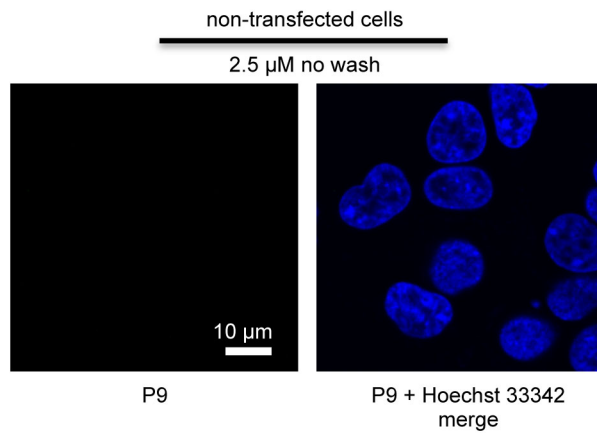


**Figure S10. P9 showed no fluorescence background without washing step in non-transfected HEK293T cells.** Non-transfected HEK293T cells were incubated with 2.5  $\mu$ M P9 for 30 min at 37 °C with no wash. Images taken by confocal microscope showed no fluorescence background (upper panel). Blue fluorescence denotes nucleus stained by Hoechst 33342. Scale bar: 10  $\mu$ m.

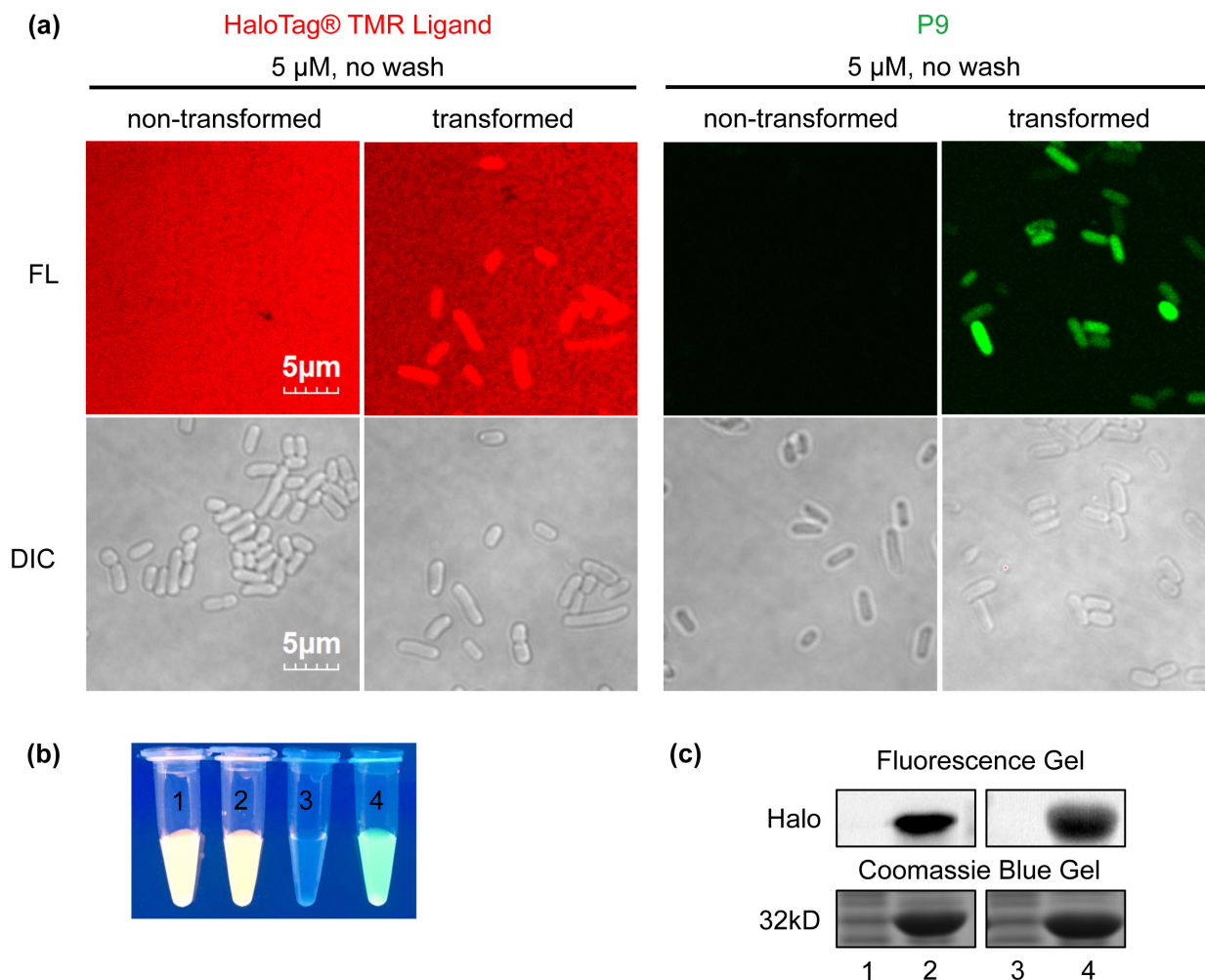


**Figure S11. No-wash imaging using P9 in *E. coli* cells.** (a) No-wash imaging of Halo protein in *E. coli* cells after incubation with 5  $\mu$ M HaloTag® TMR ligand or P9 for 30 min at 37 °C. Halo in the cytoplasm of transformed cells can be selectively imaged by P9 (5  $\mu$ M) without a wash step (the 4<sup>th</sup> lane). Non-transformed cells showed no fluorescence signal using P9 (the 3<sup>rd</sup> lane). In contrast, the HaloTag® TMR ligand (5  $\mu$ M) exhibited high fluorescence background without inclusion of washing steps in both non-transformed (the 1<sup>st</sup> lane) and transformed (the 2<sup>nd</sup> lane) *E. coli* cells. Images were taken by a confocal microscope with a scale bar of 5  $\mu$ m. (b) Fluorescence image of *E. coli* cells in solution with 5  $\mu$ M HaloTag® TMR ligand (1: non-transformed and 2: transformed) or 5  $\mu$ M P9 (3: non-transformed and 4: transformed). P9 exhibited no fluorescence background when incubating with non-transformed *E. coli* cells. (c) Covalent and selective labeling of Halo in *E. coli* cells by HaloTag® TMR ligand (1: non-transformed and 2: transformed) or P9 (3: non-transformed and 4: transformed). Total protein concentration of all lysate samples were normalized by Bradford assay (0.1 mg/mL). Fluorescence and coomassie blue SDS-Page gels were scanned using Biorad Gel Doc EZ imager.



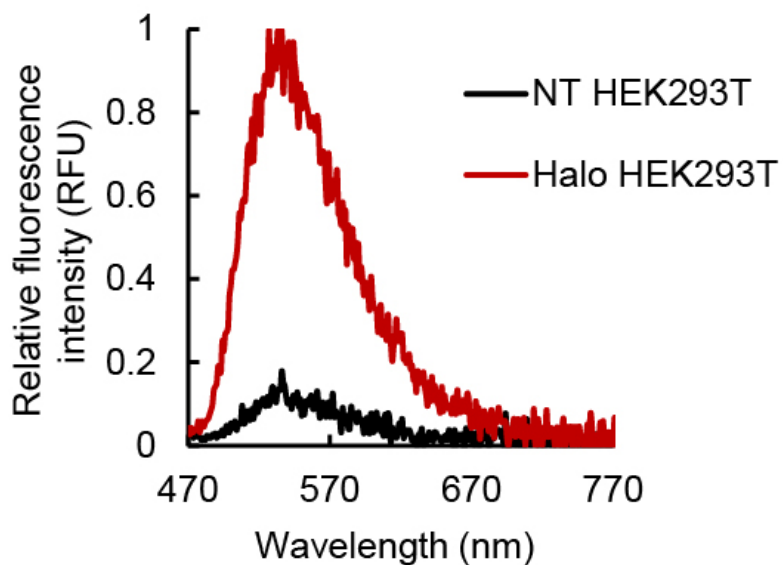


**Figure S13. Fluorescence emission spectra of P9 treated non-transfected and Halo transfected HEK293T cells.** HEK293T cells were non-transfected or transiently transfected with Halo for 24 h in 6-well plate. P9 (10  $\mu$ M) were introduced in the media directly and incubated for 30 min at 37 °C. Cells were harvested and resuspended in DPBS buffer. The cell density was normalized to  $4 \times 10^6$  cells/mL. Fluorescence emission spectra were measured by Tecan M1000Pro plate reader (excitation at 450 nm).

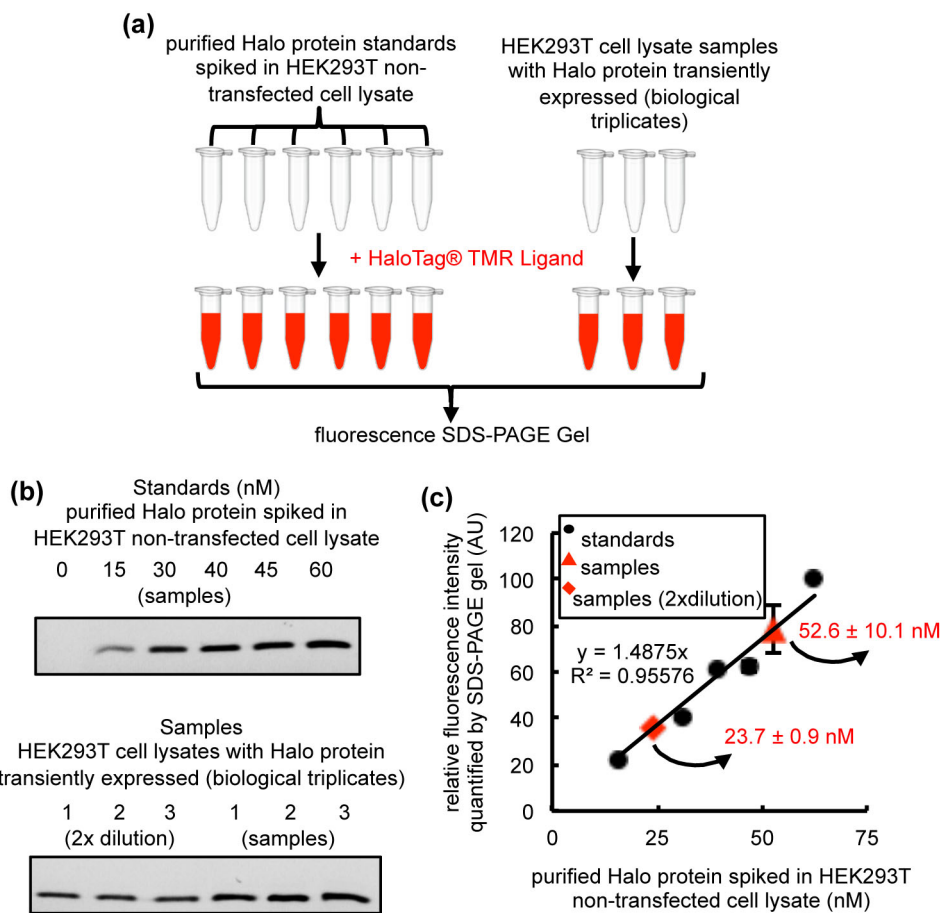


**Figure S14. Fluorescence SDS-Page gel quantification of Halo protein expression level in transiently transfected HEK293T cell lysate using HaloTag® TMR ligand.** (a) Flow chart to quantify Halo protein expression level in transfected cell lysate with HaloTag® TMR Ligand. To prepare standard samples (15 nM to 60 nM) and generate standard curve, purified Halo protein was spiked into non-transfected HEK293T cell lysate (0.2 mg/mL). Halo protein was transiently transfected in HEK293T cells for 36 h to generate test samples. Cells were harvested and lysed by sonication. Lysates were prepared as 1X dilution (0.2 mg/mL) and 2X dilution (0.1 mg/mL). To determine the concentration of Halo protein in transfected samples, both the standard samples and test samples were incubated with HaloTag® TMR Ligand (500 nM) for 2 h. Samples were resolved by electrophoresis using SDS-Page gel. Fluorescence was quantified by the intensity of Halo-TMR ligand bands. (b) Fluorescence SDS-Page gel of standards of purified Halo protein in non-transfected lysate and test samples of Halo transfected lysates. (c) Standard curve of purified Halo protein in non-transfected lysate (black dots). Concentration of Halo protein in transfected lysate was determined by fitting the standard curve. Red triangle denotes 1X dilution samples and red diamond is 2X dilution samples. All experiments were performed in biological triplicate. Error bars are standard deviation.

Fluorophores	Ground State Structure	Proposed Excited State Structure
acrylodan		
coumarin		
dansyl chloride		
naphthalimide		
dapoxyl		

**Figure S15: The dimethylamino group is commonly found in several classes of push-pull fluorophores.** These fluorophores are potential scaffolds that can utilize cation- $\pi$  interactions to enable fluorogenic probes for Halo-tag and other protein tags.



**Table S1.** Data collection and refinement statistics for the x-ray crystal structures of Halo (apo) and the Halo • P9 conjugate.

	<b>Halo</b>	<b>Halo • P9</b>
<b>Data Collection</b>		
Wavelength	0.97857 Å	0.97857 Å
Space group	$P2_12_12_1$	$P2_1$
Cell dimensions		
a, b, c (Å)	69.08, 94.63, 99.99	49.94, 69.12, 83.90
$\alpha$ , $\beta$ , $\gamma$ (°)	90.00, 90.00, 90.00	90.00, 94.67, 90.00
Resolution (Å)	50.00-1.35 (1.37-1.35)	50.00-1.92 (1.95-1.92)
No. observations	144106 (7088)	42358 (1810)
Unique reflections	144217	43590
$R_{\text{merge}}$	0.069 (0.793)	0.094 (0.511)
$\langle I/\sigma \rangle$	26.9 (2.3)	11.7 (1.9)
$CC_{1/2}$	0.792	0.761
Completeness (%)	99.9 (99.5)	97.2 (84.9)
Redundancy	7.1 (6.7)	3.7 (3.2)
<b>Refinement</b>		
Resolution (Å)	50.00 - 1.35	50.00 - 1.92
No. reflections	133179	33903
$R_{\text{work}} / R_{\text{free}}$	0.188/0.196	0.269/0.287
No. atoms		
protein	4668	4693
ion/ligand	23	64
water	437	72
<i>B</i> -factors		
protein	14.0	26.2
ion/ligand	24.2	24.6
water	23.6	18.4
r.m.s. deviations		
bond lengths (Å)	0.004	0.005
bond angles (°)	0.997	0.960
Ramachandran statistics (%)		
favored	96.7	95.2
outliers	0.0	0.17
Protein databank ID code		

**Table S2. Spectroscopic properties of fluorogenic probes and Halo protein conjugates.** Quantum yields of the Halo-P9, P8 or P4 conjugate were measured following reported protocol<sup>(1)</sup> using fluorescein in 0.1 M NaOH aqueous solution ( $\Phi = 0.93$ )<sup>(2)</sup> as a standard. Molar extinction coefficients, excitation/emission wavelengths were measured by Agilent Cary-Series UV-Vis Spectrophotometer following Beer-Lambert Law. Other commonly used imaging tools, such as Fluorescein, EGFP and Alexa Fluor 488 were adopted from literature for comparison purpose. All measurements were performed in triplicate.

<b>Dyes or Fluorescent Proteins</b>	$\lambda_{\text{ex}}/\lambda_{\text{em}}$ (nm)	<b>absorptivity</b> ( $\epsilon$ , $\text{M}^{-1}\cdot\text{cm}^{-1}$ )	<b>quantum yield</b> ( $\Phi$ )
Halo-P9	450/530	5100	0.47±0.03
Halo-P8	440/535	7800	0.37±0.03
Halo-P4	423/545	4100	0.16±0.01
Fluorescein	490/525	76900	0.93
EGFP	488/507	56000	0.60
Alexa Fluor 488	496/519	71000	0.92 <sup>(3)</sup>

**Table S3: The ground state geometry of the Trp141-P9 cluster. The total energy at this geometry is -2935.55046566 Hartree. The number of imaginary frequency is 0.**

Atom	X(Å)	Y(Å)	Z(Å)
C	-8.77074700	-1.75439000	1.56298000
C	-7.59322600	-0.80637300	1.28162600
O	-7.27605200	0.04773600	2.11186500
N	-6.94699100	-0.96332500	0.12565800
C	-5.83170300	-0.09598800	-0.26351800
C	-5.18639600	-0.58779000	-1.56588600
C	-4.30344500	-1.79326700	-1.41274900
C	-4.66818200	-3.03504800	-0.97694900
N	-3.58181600	-3.87691400	-0.98045300
C	-2.48734100	-3.18581500	-1.43060800
C	-2.90601100	-1.87060000	-1.71709800
C	-1.96473300	-0.95149300	-2.19647500
C	-0.65444100	-1.37139800	-2.37623400
C	-0.26847600	-2.68867300	-2.08382300
C	-1.16733200	-3.60757100	-1.61028500
C	-6.29538700	1.34948300	-0.46167900
O	-7.41899900	1.58158000	-0.91125600
N	-5.43262800	2.32845200	-0.12404600
C	-5.71217300	3.71655600	-0.49693500
C	-4.48575700	4.47481000	0.02044400
C	-3.97946100	3.64645400	1.14732700
C	-4.25146300	2.22331700	0.75416400
S	2.31851300	2.43510900	-0.92349100
C	1.31144500	1.26814800	-0.06766100
C	1.72721600	-0.05495200	0.10756400
C	0.90700400	-0.97065300	0.76614100
C	-0.37098900	-0.61210400	1.23450600
C	-0.75608300	0.73209300	1.05926600
C	0.05980100	1.64777300	0.41592400
N	-1.23487200	-1.56343600	1.75276900
C	-0.77498400	-2.44059200	2.82308500
C	-2.64066500	-1.22413700	1.84643700
N	1.39303700	-2.31644000	0.73479700
N	2.91908400	-0.61015600	-0.42574700
S	3.06264900	-2.17473400	0.31443600
N	3.58949600	2.67139500	0.12306200
C	4.90480500	2.90682400	-0.44420800
C	5.98987400	2.15679600	0.33881200
N	7.25444900	2.38319700	-0.10360100
C	8.32024900	1.45288200	0.27182800
C	8.27571200	0.16853600	-0.55567400
C	8.00397900	-1.04375700	0.32054900
C	3.27235000	3.42019800	1.33714300
O	2.86557600	1.81090500	-2.12864600
O	1.53170300	3.65940100	-1.07679600
O	5.73094100	1.41598800	1.27843800
C	7.28879000	-2.16082100	-0.42685600

C	7.76436200	-3.52982000	0.03894700
C	7.59790400	-3.70437000	1.53350700
H	-5.98132200	-0.75915600	-2.30334200
H	-4.58163300	0.23528700	-1.96244500
H	-5.63366600	-3.39982800	-0.65375200
H	-3.59300400	-4.84596600	-0.69773300
H	-2.25097200	0.07275100	-2.42156600
H	0.08624900	-0.67180800	-2.75285300
H	-0.87433700	-4.63054700	-1.39162500
H	0.75432600	-2.99963300	-2.28873800
H	-5.08683000	-0.14210200	0.53485200
H	-7.34582600	-1.56262600	-0.58341400
H	-3.73509900	4.53376900	-0.77753600
H	-4.73407600	5.49855400	0.31230400
H	-2.91976400	3.81219900	1.36304200
H	-4.53553800	3.88033000	2.06405000
H	-3.40657500	1.79280500	0.20110300
H	-4.46299400	1.57997700	1.61183800
H	-6.63589500	4.05600500	-0.01181600
H	4.91647600	2.53493300	-1.47167000
H	5.14208300	3.97971200	-0.47811900
H	-1.70360700	1.07008300	1.45837100
H	-0.26268700	2.67681700	0.30164900
H	-0.86397700	-1.95079600	3.80445800
H	-1.39012700	-3.34546900	2.83120700
H	0.26250400	-2.72751100	2.65693500
H	-2.96897900	-0.76662000	0.91026900
H	-3.21136600	-2.14687200	1.98281100
H	-2.87169700	-0.54975300	2.68698800
H	0.85077500	-2.84474800	0.04605500
H	2.89289400	-0.62776800	-1.44467400
H	9.28369300	1.96353200	0.18942300
H	8.14339400	1.24786000	1.33007600
H	7.46995000	0.27515900	-1.29080400
H	9.19996000	0.02312600	-1.12700300
H	8.95604300	-1.40632800	0.73012600
H	7.39615500	-0.73912100	1.17946900
H	2.33006600	3.06202900	1.75830000
H	3.19900100	4.49821300	1.14868400
H	4.06242400	3.22187600	2.06239200
H	7.47425400	-2.06998200	-1.50590600
H	6.20475800	-2.06856700	-0.28706600
H	7.21467800	-4.32073200	-0.48846900
H	8.82263300	-3.65063800	-0.23118800
H	6.55360000	-3.54374000	1.83213700
H	8.21445300	-3.00030700	2.10176300
H	7.88004400	-4.71457300	1.85414000
H	-8.96457000	-2.45949400	0.74966200
H	-8.55182800	-2.31239000	2.47803800
H	-9.66577200	-1.15129500	1.73992300

H	-5.85149500	3.80226000	-1.57821800
H	7.36398500	2.88525000	-0.97484700

**Table S4: The relaxed geometry of the Trp141-P9 upon excitation. The total energy at this geometry is -2935.52294303 Hartree.**

Atom	X(Å)	Y(Å)	Z(Å)
C	-8.82612500	-1.75498200	1.60321700
C	-7.63719200	-0.82473300	1.31077000
O	-7.31653900	0.04250900	2.12592000
N	-6.98530700	-1.01122400	0.16240400
C	-5.85864300	-0.16296200	-0.23673100
C	-5.21029500	-0.68740800	-1.52473400
C	-4.34071700	-1.89841600	-1.34191600
C	-4.72091500	-3.12750300	-0.88391000
N	-3.64323600	-3.98022500	-0.86358600
C	-2.53890700	-3.30935500	-1.32023200
C	-2.94225200	-1.99594400	-1.63553600
C	-1.98858800	-1.09615600	-2.12693100
C	-0.68156500	-1.53281300	-2.28977100
C	-0.31093500	-2.84777600	-1.96857100
C	-1.22218700	-3.74795900	-1.48289300
C	-6.30631300	1.28268000	-0.46653600
O	-7.42462300	1.51712700	-0.92796100
N	-5.43572700	2.25938700	-0.14279200
C	-5.69865800	3.64255300	-0.54502200
C	-4.46783200	4.39852100	-0.03482000
C	-3.97719800	3.58772300	1.11158000
C	-4.26129600	2.15983200	0.74500900
S	2.42076400	2.56968400	-1.02137600
C	1.29187400	1.44936000	-0.39746400
C	1.70835200	0.09946700	-0.10860300
C	0.90709900	-0.76230100	0.61698900
C	-0.32615000	-0.38942800	1.20543600
C	-0.69613100	0.95481900	0.98018300
C	0.07422600	1.83451800	0.22703800
N	-1.06004300	-1.35220200	1.93466800
C	-0.54672200	-1.61762500	3.27879500
C	-2.49991300	-1.15886800	1.92802500
N	1.39266500	-2.06012000	0.62129700
N	2.79589300	-0.53429900	-0.70652900
S	2.83581000	-2.16770300	-0.27328800
N	3.64192900	2.74962400	0.12771000
C	4.99774200	3.00410700	-0.31305200
C	5.99533000	2.05940500	0.37067200
N	7.27748500	2.21054600	-0.04164700
C	8.30474000	1.25275700	0.36023900
C	8.25219200	-0.04734100	-0.44188900
C	7.96252800	-1.23911100	0.45647300
C	3.24427100	3.37972800	1.37803400
O	3.11917700	1.95438000	-2.16750800
O	1.73747800	3.85200600	-1.25060200
O	5.65966500	1.24839000	1.22659400
C	7.24067100	-2.36356200	-0.27323500

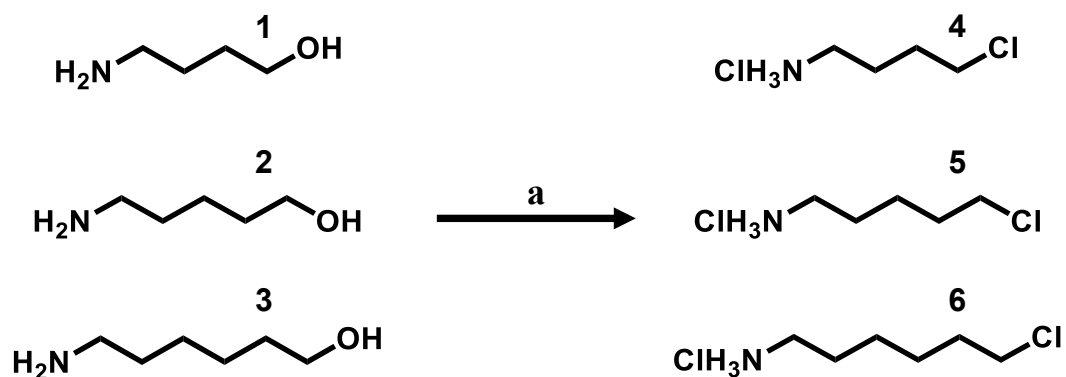
C	7.69922700	-3.72774300	0.22278400
C	7.52153600	-3.87075900	1.71939900
H	-6.00223800	-0.86533900	-2.26382700
H	-4.59461300	0.12148500	-1.93363100
H	-5.69211300	-3.47597300	-0.55983800
H	-3.66614500	-4.94328300	-0.56173800
H	-2.26288200	-0.07375900	-2.37420100
H	0.06863300	-0.84839900	-2.67535300
H	-0.94107600	-4.76927700	-1.24200700
H	0.70985600	-3.17319300	-2.16079000
H	-5.11949400	-0.20111700	0.56741500
H	-7.38576200	-1.62049500	-0.53721400
H	-3.71157500	4.43395300	-0.82889500
H	-4.70748500	5.43034300	0.23500600
H	-2.91724000	3.74699900	1.33088100
H	-4.53663300	3.84544900	2.01983100
H	-3.41741400	1.70994700	0.20614000
H	-4.48480500	1.53592700	1.61392500
H	-6.62190300	4.00094300	-0.07278900
H	5.05628500	2.84260000	-1.39171300
H	5.29216900	4.04621200	-0.12001100
H	-1.61540700	1.32731800	1.41957300
H	-0.26594300	2.85772500	0.09957500
H	-0.71396100	-0.76804000	3.96210000
H	-1.04799100	-2.49973500	3.69036700
H	0.52612400	-1.82093400	3.23307100
H	-2.83737500	-0.99218700	0.90162600
H	-2.98419400	-2.06442600	2.30758000
H	-2.82999600	-0.31379000	2.55778700
H	0.71764700	-2.82350300	0.55917100
H	3.05316500	-0.26096700	-1.65904500
H	9.27381000	1.75184500	0.27392700
H	8.11901300	1.07063800	1.42113100
H	7.45225700	0.05274600	-1.18423400
H	9.17852400	-0.21347700	-1.00415000
H	8.90821600	-1.60306200	0.87938400
H	7.35243700	-0.91127000	1.30518000
H	2.27042500	2.99406500	1.69145000
H	3.18667300	4.47361500	1.29490700
H	3.97599400	3.10879400	2.14200800
H	7.43387900	-2.29614200	-1.35264300
H	6.15677800	-2.25757000	-0.14238800
H	7.14481300	-4.52341100	-0.29238500
H	8.75789200	-3.86463100	-0.03798000
H	6.47706500	-3.69364300	2.00795200
H	8.14166100	-3.16178000	2.27756200
H	7.79127100	-4.87717100	2.06188400
H	-9.02201600	-2.47416800	0.80282700
H	-8.61873200	-2.29681000	2.53059600
H	-9.71602200	-1.13944900	1.76228800

H	-5.83025000	3.70808200	-1.62868200
H	7.45909500	2.79454000	-0.84599600

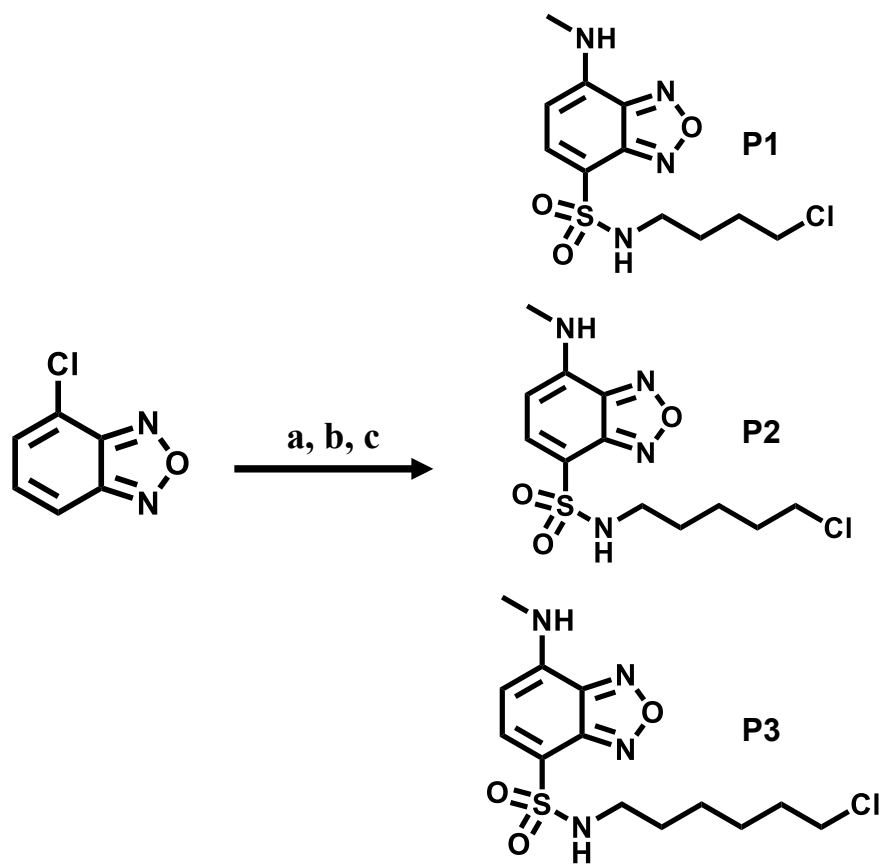


## **General synthetic and Chromatographic Methods.**

All reagents and anhydrous solvents of commercial grade were used as received unless otherwise stated. Reactions were monitored by thin layer chromatography (TLC) analysis using Silicycle® glass sheets precoated with silica gel 60 Å with detection by UV-absorption (254 nm or 365 nm). Flash column chromatography was performed using Silica Flash® F60 silica gel in the indicated solvent mixture. <sup>1</sup>H NMR and <sup>13</sup>C NMR spectra were obtained on a Bruker NMR (400/100 MHz) spectrometer in the given solvents. Chemical shifts are reported as δ-values in ppm relative to the CDCl<sub>3</sub> residual solvent peak or tetramethylsilane (TMS) as an internal standard. Coupling constants are provided in Hz. All given <sup>13</sup>C spectra are proton-decoupled. High resolution mass spectra were recorded with a Waters Q-TOF Premier quadrupole/time-of-flight (TOF) mass spectrometer.



**Scheme S1. Synthesis of linkers for the probes.** Commercially available amino alcohols 1, 2, 3, and 4 were used to make linkers with different length, generating chlorinated linkers 5, 6, 7, 8. Conditions (a)  $\text{SOCl}_2$  (4.5 eq), Toluene, 2.5 h, 60 °C. Removal of residual solvent under reduced pressure yielded crude hygroscopic solid. The product was carried on to the next step without further purification.



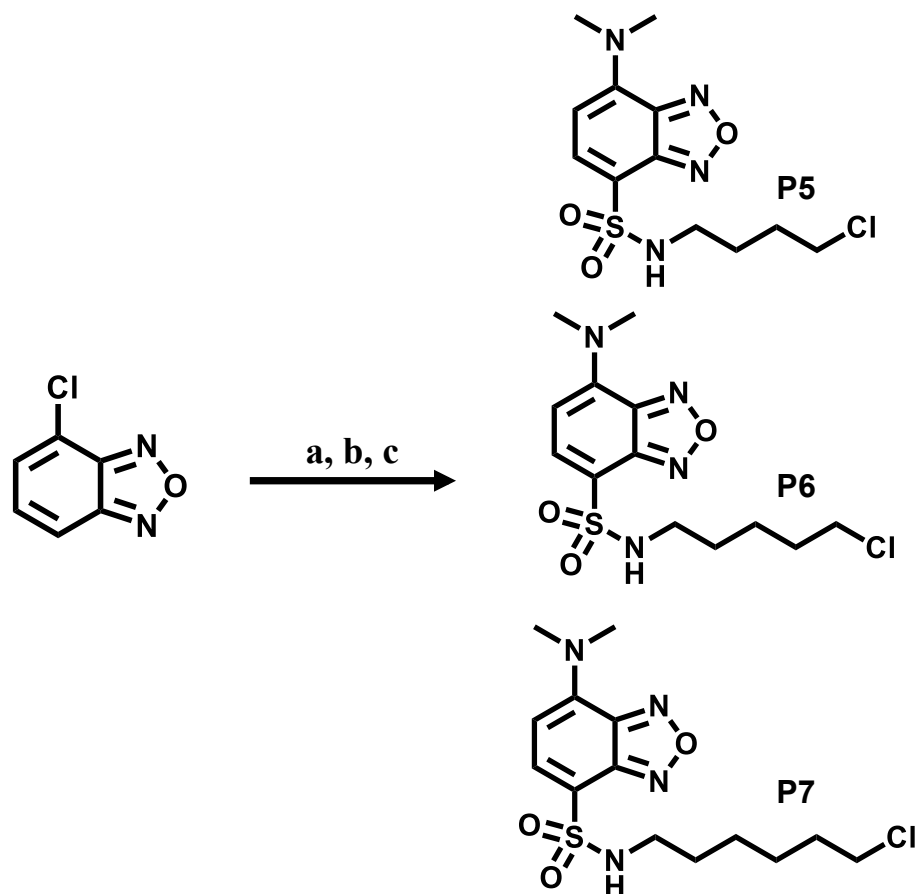
**Scheme S2. Synthesis of SBD fluorogenic probes.** Commercially available 4-Chloro-2,1,3-benzoxadiazole was used as the precursor for the synthesis of SBD fluorophores. Conditions (a) HSO<sub>3</sub>Cl (7 eq), 6 h, 150 °C; overnight, RT. (b) 4, 5, 6 respectively (1 eq), triethylamine (2 eq), dichloromethane, 1 h, RT. (c) 40% aq. methylamine (10 eq), dichloromethane, overnight, RT. The reaction mixture was quenched by water and extracted with DCM. The organic fraction was dried *in vacuo*. Compounds were further purified by flash chromatography using 1:1 ethyl acetate: hexane as eluent, generating P1, P2, and P3.

**P1.** Orange crystallized solid. ( $R_f=0.47$ , 1:1 EA:Hexane) <sup>1</sup>H NMR (400 MHz, MeOD)  $\delta$  7.91 (d,  $J = 8.1$  Hz, 1H), 6.17 (d,  $J = 8.1$  Hz, 1H), 3.48 (t,  $J = 6.5$  Hz, 2H), 3.05 (s, 3H), 2.94 (t,  $J = 6.8$  Hz, 2H), 1.77 – 1.65 (m, 2H), 1.63 – 1.50 (m, 2H). <sup>13</sup>C NMR (101 MHz, DMSO)  $\delta$  145.95,

144.93, 140.13, 137.88, 108.36, 100.45, 44.93, 41.54, 29.16, 26.48, 24.97. HRMS for  $[M+Na]^+$ :  
Calcd, 341.0451, Obsd, 341.0465.

**P2.** Light orange crystallized solid. ( $R_f=0.48$ , 1:1 EA:Hexane)  $^1H$  NMR (400 MHz,  $CDCl_3$ )  $\delta$  8.24 (q,  $J = 4.9$  Hz, 1H), 7.82 (t,  $J = 8.6$  Hz, 1H), 7.55 (t,  $J = 5.8$  Hz, 1H), 6.16 (d,  $J = 8.2$  Hz, 1H), 3.49 (t,  $J = 6.6$  Hz, 2H), 2.94 (d,  $J = 4.8$  Hz, 3H), 2.79 (dd,  $J = 12.7, 6.5$  Hz, 2H), 1.61 – 1.46 (m, 2H), 1.39 – 1.14 (m, 4H).  $^{13}C$  NMR (101 MHz, DMSO)  $\delta$  145.48, 144.36, 141.51, 138.71, 110.21, 98.13, 45.19, 42.13, 31.53, 29.74, 28.30, 23.40. HRMS for  $[M+H]^+$ : Calcd. 333.0788, Obsd, 333.1255.

**P3.** Light orange crystallized solid. ( $R_f=0.5$ , 1:1 EA:Hexane).  $^1H$  NMR (400 MHz,  $CDCl_3$ )  $\delta$  7.95 (d,  $J = 7.9$  Hz, 1H), 6.10 (d,  $J = 7.9$  Hz, 1H), 5.78 (d,  $J = 4.2$  Hz, 1H), 4.92 (t,  $J = 5.7$  Hz, 1H), 3.52-3.44 (m, 2H), 3.12 (d,  $J = 5.2$  Hz, 3H), 2.97-2.87(m, 2H), 1.81 – 1.60 (m, 4H), 1.55 – 1.41 (m, 2H), 1.39 – 1.19 (m, 2H).  $^{13}C$  NMR (101 MHz, DMSO)  $\delta$  145.45, 144.33, 141.46, 138.70, 110.24, 98.11, 45.18, 42.16, 31.87, 29.71, 28.80, 25.71, 25.17. HRMS for  $[M+Na]^+$ :  
Calcd, 369.0766, Obsd, 369.0764.



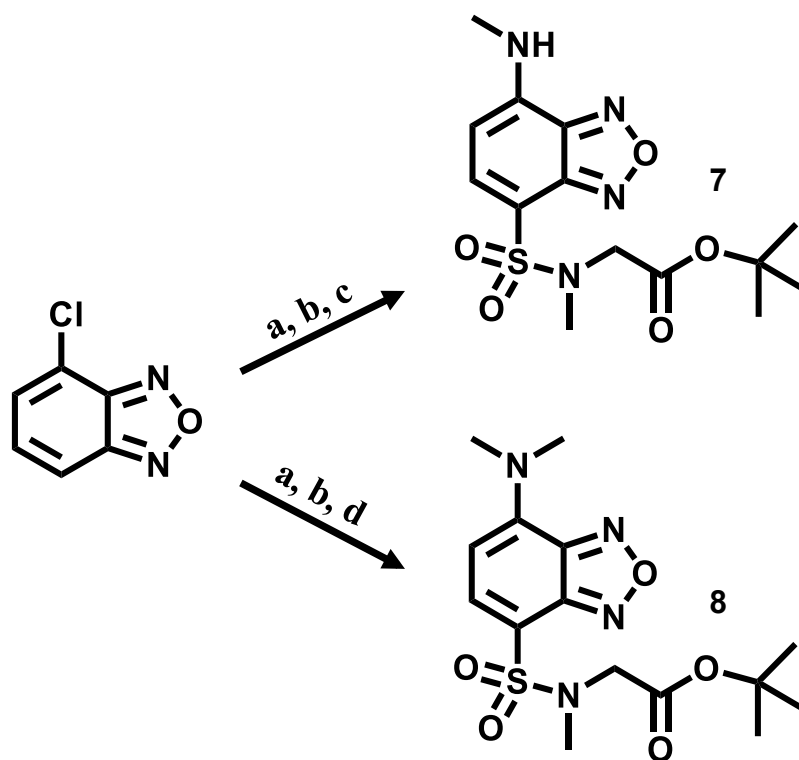
**Scheme S3. Synthesis of SBD fluorogenic probes with dimethylamine donor.** Commercially available 4-Chloro-2,1,3-benzoxadiazole was used as the precursor for the fluorogenic probes. Condition (a)  $\text{HSO}_3\text{Cl}$  (7 eq), 6 h, 150 °C; overnight, RT. (b) 4, 5, 6 respectively (1 eq), triethylamine (2 eq), Dichloromethane, 1 h, RT. (c) 40% aq. dimethylamine (10 eq), dichloromethane, overnight, RT. The reaction mixture was quenched by water and extracted with DCM. The organic fraction was dried in *vacuo*. Compounds were further purified by flash chromatography using 1:1 ethyl acetate: hexane as eluent. P5, P6, and P7 were obtained

**P5.** Orangish yellow crystallized solid. ( $R_f=0.65$ , 1:1 EA:Hexane).  $^1\text{H}$  NMR (400 MHz,  $\text{CDCl}_3$ )  $\delta$  7.82 (d,  $J = 8.2$  Hz, 1H), 5.98 (d,  $J = 8.3$  Hz, 1H), 5.14 (t,  $J = 6.1$  Hz, 1H), 3.48 – 3.34 (m, 8H), 2.946-2.849 (m, 2H), 1.77 – 1.66 (m, 2H), 1.63 – 1.51 (m, 2H).  $^{13}\text{C}$  NMR (101 MHz, DMSO)  $\delta$

146.08, 144.87, 142.59, 137.53, 109.86, 101.54, 44.90, 42.21, 41.55, 29.15, 26.49. HRMS for  $[M+Na]^+$ : Calcd, 355.0608, Obsd, 355.0610.

**P6.** Orangish yellow crystallized solid. ( $R_f=0.65$ , 1:1 EA:Hexane).  $^1H$  NMR (400 MHz,  $CDCl_3$ )  $\delta$  7.89 (d,  $J = 8.2$  Hz, 1H), 6.03 (d,  $J = 8.3$  Hz, 1H), 4.87 (t,  $J = 6.0$  Hz, 1H), 3.51 (s, 6H), 3.46 (t,  $J = 6.6$  Hz, 2H), 2.941-2.85 (m, 2H), 1.74 – 1.64 (m, 2H), 1.538-11.45 (m, 2H), 1.45 – 1.35 (m, 2H).  $^{13}C$  NMR (101 MHz,  $CDCl_3$ )  $\delta$  146.30, 145.17, 143.42, 137.98, 109.66, 101.19, 44.80, 43.08, 42.70, 32.01, 28.95, 23.92. HRMS for  $[M+Na]^+$ : Calcd, 369.0764, Obsd, 369.2034.

**P7.** Orangish yellow crystallized solid. ( $R_f=0.67$ , 1:1 EA:Hexane).  $^1H$  NMR (400 MHz,  $CDCl_3$ )  $\delta$  7.89 (d,  $J = 8.2$  Hz, 1H), 6.03 (d,  $J = 8.3$  Hz, 1H), 4.84 (t,  $J = 6.2$  Hz, 1H), 3.51 (s, 6H), 3.48 (t,  $J = 6.6$  Hz, 2H), 2.89 (dd,  $J = 13.4, 6.8$  Hz, 2H), 1.73 – 1.64 (m, 2H), 1.51 – 1.42 (m, 2H), 1.39 – 1.23 (m, 4H).  $^{13}C$  NMR (101 MHz,  $CDCl_3$ )  $\delta$  146.28, 145.14, 143.36, 137.95, 109.63, 101.17, 44.99, 43.11, 42.68, 32.37, 29.38, 26.32, 25.82. HRMS for  $[M+H]^+$ : Calcd. 361.1101, Obsd, 361.1140.



**Scheme S4. Synthesis of SBD fluorogenic probes with rigid extended linker intermediate.**

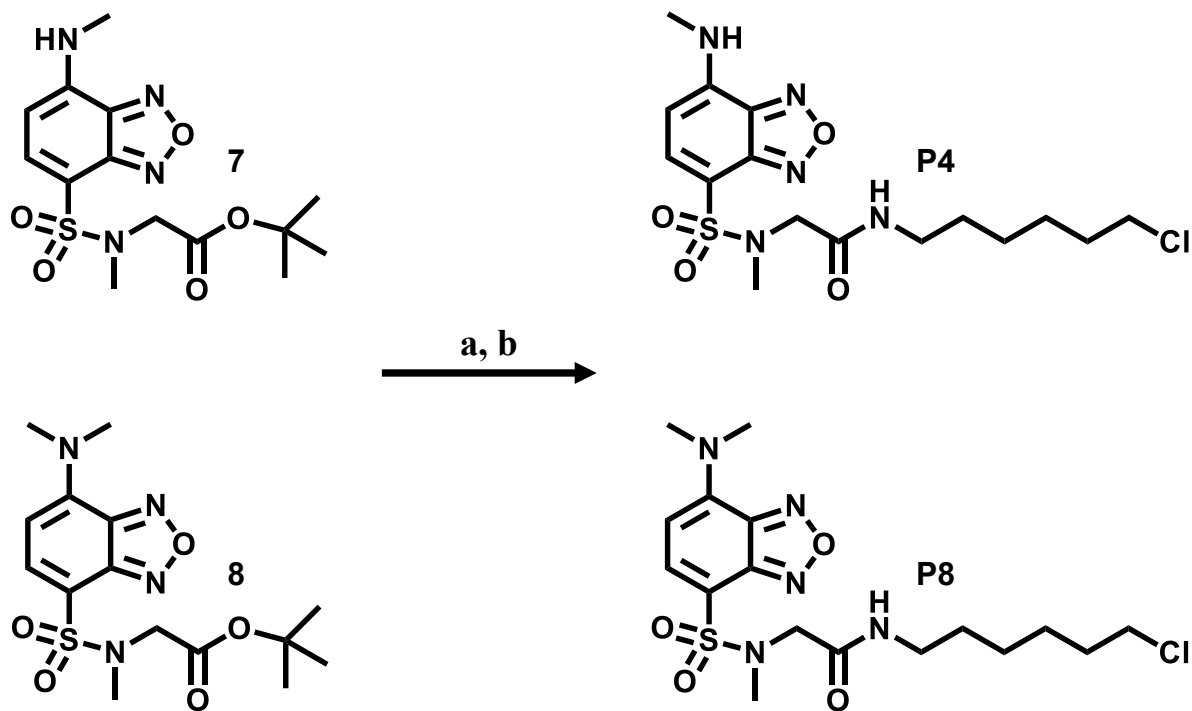
Commercially available 4-Chloro-2,1,3-benzoxadiazole was used as the precursor. Condition (a) HSO<sub>3</sub>Cl (7 eq), 6 h, 150 °C; overnight, RT. (b) Sarcosine tert-butyl ester hydrochloride (1 eq), triethylamine (1 eq), Dichloromethane, overnight, RT. (c) 40% aq. methylamine (10 eq), dichloromethane, overnight, RT. (d) 40% aq. dimethylamine (10 eq), dichloromethane, overnight, RT.

7. Orange solid. ( $R_f=0.55$ , 1:1 EA:Hexane). <sup>1</sup>H NMR (400 MHz, CDCl<sub>3</sub>) δ 8.35-8.27 (m, 1H), 7.82 (d,  $J = 8.1$  Hz, 1H), 6.13 (d,  $J = 8.1$  Hz, 1H), 4.02 (s, 2H), 2.94 (s, 3H), 2.85 (s, 3H), 1.23 (s, 9H). <sup>13</sup>C NMR (101 MHz, DMSO) δ 167.71, 146.08, 144.35, 141.90, 139.31, 108.02, 98.12, 81.11, 51.11, 35.24, 29.70, 27.67, 27.44, 27.21.

8. Reddish orange syrup. ( $R_f=0.6$ , 1:1 EA:Hexane). <sup>1</sup>H NMR (400 MHz, CDCl<sub>3</sub>) δ 7.78 (d,  $J = 8.3$  Hz, 1H), 6.18 (d,  $J = 8.4$  Hz, 1H), 4.02 (s, 2H), 3.41 (s, 6H), 2.84 (s, 3H), 1.27 (s, 9H). <sup>13</sup>C

NMR (101 MHz, DMSO)  $\delta$  167.71, 146.61, 144.79, 142.79, 138.13, 107.68, 101.48, 81.05, 51.11, 42.17, 35.19, 27.44.



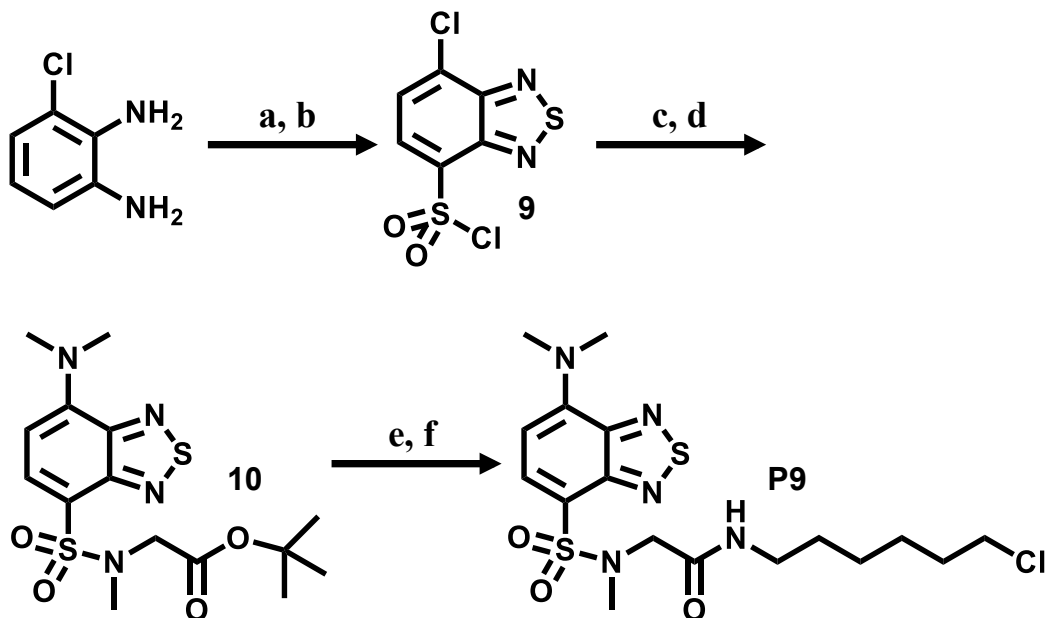


**Scheme S5. Synthesis of SBD fluorogenic probes with rigid extended linker.** Intermediate 7 and 8, after NMR characterization was subjected to further reaction to get Probe 4 and Probe 8. Conditions (a): Trifluoroacetic acid (excess), 2 h, RT. (b) 6 (2 eq), 1-Hydroxybenzotriazole hydrate (HOBt) (3 eq), triethylamine (4 eq), N-(3-Dimethylaminopropyl)-N'-ethylcarbodiimide hydrochloride (EDC) (3 eq), overnight, RT. The reaction mixture was quenched by water and extracted with DCM. The organic fraction was dried in vacuo. Compounds were further purified by flash chromatography using 1:1 EA:Hexane to 100% ethyl acetate as eluent. P4 and P8 was obtained respectively.

**P4.** Orangish yellow solid. ( $R_f=0.6$ , 1:1 EA:Hexane). <sup>1</sup>H NMR (400 MHz, CDCl<sub>3</sub>)  $\delta$  7.99 (d,  $J = 8.0$  Hz, 1H), 7.02-6.92 (m, 1H), 6.13 (d,  $J = 8.0$  Hz, 1H), 6.09-5. (m, 1H), 3.89 (s, 2H), 3.53 (t,  $J = 6.6$  Hz, 2H), 3.31 (dd,  $J = 13.0, 6.6$  Hz, 2H), 3.14 (d,  $J = 5.1$  Hz, 3H), 2.85 (s, 3H), 1.77 (dt,  $J = 13.8, 6.7$  Hz, 2H), 1.63 (m, 2H), 1.51 – 1.41 (m, 2H), 1.41 – 1.30 (m, 2H). <sup>13</sup>C NMR (101

MHz, DMSO)  $\delta$  167.10, 146.11, 144.33, 141.95, 139.80, 107.25, 98.20, 52.11, 45.31, 38.40, 35.98, 32.00, 29.73, 28.79, 25.98, 25.58. HRMS for  $[M+Na]^+$ : Calcd, 440.1135, Obsd, 440.1123.

**P8.** Reddish Orange solid. ( $R_f=0.6$ , 1:1 EA:Hexane).  $^1H$  NMR (400 MHz,  $CDCl_3$ )  $\delta$  7.88 (d,  $J = 8.4$  Hz, 1H), 7.12-7.019 (m, 1H), 6.02 (d,  $J = 8.4$  Hz, 1H), 3.86 (s, 2H), 3.556-3.446 (m, 8H), 3.33 – 3.24 (m, 2H), 2.79 (s, 3H), 1.80 – 1.68 (m, 2H), 1.61 – 1.49 (m, 2H), 1.484-1.387 (m, 2H), 1.39 – 1.28 (m, 2H).  $^{13}C$  NMR (101 MHz,  $CDCl_3$ )  $\delta$  168.16, 146.65, 145.10, 144.03, 139.83, 106.05, 101.49, 53.51, 45.04, 42.93, 39.37, 36.69, 32.46, 29.28, 26.52, 26.15. HRMS for  $[M+H]^+$ : Calcd, 432.1472, Obsd, 432.1446.



**Scheme S6. Synthesis of sulfonated SBD fluorogenic probe molecule.** Commercially available 3-Chloro-1,2-diaminobenzene was used as the precursor and subjected to multiple reaction pathways: (a) N-Thionylaniline (9 eq), Toluene, 3 h, 130 °C. (b) HSO<sub>3</sub>Cl (7 eq), 6 h, 150 °C; overnight, RT. Intermediate 11 was purified and characterized before subjected to further reactions. (c) Sarcosine tert-butyl ester hydrochloride (1 eq), triethylamine (1 eq), dichloromethane, overnight, RT. (d) 40% aq. dimethylamine (10 eq), dichloromethane, overnight, RT. (e) Trifluoroacetic acid (excess), 2 h, RT. (f) 5 (2 eq), 1-Hydroxybenzotriazole hydrate (HOBt) (3 eq), triethylamine (4 eq), N-(3-Dimethylaminopropyl)-N'-ethylcarbodiimide hydrochloride (EDC) (3 eq), overnight, RT. The reaction mixture was quenched by water and extracted with DCM. The organic fraction was dried in *vacuo*. Compounds were further purified by flash chromatography using 1:1 EA:Hexane to 100% ethyl acetate as eluent.

**9.** Light brown solid. ( $R_f=0.8$ , 100% Ethyl Acetate). <sup>1</sup>H NMR (400 MHz, CDCl<sub>3</sub>) δ 8.35 (d,  $J = 7.8$  Hz, 1H), 7.84 (d,  $J = 7.8$  Hz, 1H). <sup>13</sup>C NMR (101 MHz, DMSO) δ 153.57, 148.64, 135.63, 133.73, 132.21, 127.32.

**10.** Reddish orange solid. ( $R_f=0.72$ , 1:1 EA:Hexane). <sup>1</sup>H NMR (400 MHz, CDCl<sub>3</sub>) δ 8.04 (d,  $J = 8.4$  Hz, 1H), 6.32 (d,  $J = 8.5$  Hz, 1H), 4.14 (s, 2H), 3.46 (s, 6H), 2.92 (s, 3H), 1.34 (s, 9H). <sup>13</sup>C

NMR (101 MHz, CDCl<sub>3</sub>)  $\delta$  168.37, 152.39, 148.00, 146.83, 135.25, 116.52, 103.63, 81.68, 52.35, 42.76, 35.64, 28.05.

**P9.** Deep orange crystalline solid. ( $R_f=0.7$ , 1:1 EA:Hexane). <sup>1</sup>H NMR (400 MHz, CDCl<sub>3</sub>)  $\delta$  8.12 (d,  $J = 8.5$  Hz, 1H), 7.10-7.01 (m, 1H), 6.38 (d,  $J = 8.6$  Hz, 1H), 3.96 (s, 2H), 3.57 – 3.50 (m, 8H), 3.35-3.27 (m, 2H), 2.83 (s, 3H), 1.82 – 1.72 (m, 2H), 1.61 – 1.52 (m, 2H), 1.51-1.42 (m, 2H), 1.42 – 1.31 (m, 2H). <sup>13</sup>C NMR (101 MHz, CDCl<sub>3</sub>)  $\delta$  168.76, 152.20, 147.69, 147.22, 136.93, 112.57, 103.32, 54.08, 44.98, 42.87, 39.29, 36.80, 32.40, 29.42, 26.49, 26.12. HRMS for [M+H]<sup>+</sup>: Calcd, 448.1244, Obsd, 448.1238.

## References

1. Wurth, C., Grabolle, M., Pauli, J., Spieles, M., and Resch-Genger, U. (2013) Relative and absolute determination of fluorescence quantum yields of transparent samples, *Nat. Protoc.* 8, 1535-1550.
2. Brannon, J. H., and Magde, D. (1978) Absolute Quantum Yield Determination by Thermal Blooming - Fluorescein, *J. Phys. Chem.* 82, 705-709.
3. Panchuk-Voloshina, N., Haugland, R. P., Bishop-Stewart, J., Bhalgat, M. K., Millard, P. J., Mao, F., Leung, W. Y., and Haugland, R. P. (1999) Alexa dyes, a series of new fluorescent dyes that yield exceptionally bright, photostable conjugates, *J. Histochem. Cytochem.* 47, 1179-1188.